Materials Chemistry and Physics 183 (2016) 422–429

Contents lists available at ScienceDirect

Materials Chemistry and Physics

journal homepage: www.elsevier.com/locate/matchemphys

Magnetic polymer-silica composites as bioluminescent sensors for bilirubin detection

Alexander S. Timin [a, e, *], Alexey V. Solomonov [a, b], Akiko Kumagai [c], Atsushi Miyawaki [c], Svetlana Yu Khashirova [d], Azamat Zhansitov [d], Evgeniy V. Rumyantsev [a]

[a] Inorganic Chemistry Department, Ivanovo State University of Chemistry and Technology (ISUCT), 7, Sheremetevsky prosp., 153000, Ivanovo, Russian Federation
[b] Department of Materials and Interfaces, Weizmann Institute of Science, Rehovot, 7610001, Israel
[c] Cell Function Dynamics, Brain Science Institute RIKEN, 2-1 Hirosawa, Wako-city, Saitama, 351-0198, Japan
[d] Kabardino-Balkar State University, 173 Chernyshevskogo St., Nal'chik, 360004, Kabardino-Balkaria, Russian Federation
[e] RASA Center in Tomsk, Tomsk Polytechnic University, pros. Lenina, 30, Tomsk, Russian Federation

HIGHLIGHTS

- Novel magnetic silicas grafted by guanidine containing co-polymers were prepared.
- Unag protein was effectively loaded into polymer coated silicas.
- The fluorescent properties depend on content of bilirubin.

GRAPHICAL ABSTRACT

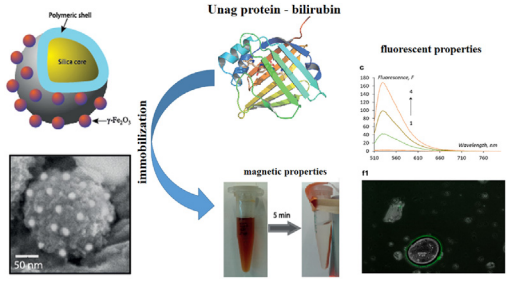

ARTICLE INFO

Article history:
Received 5 April 2016
Received in revised form
5 August 2016
Accepted 28 August 2016
Available online 8 September 2016

Keywords:
Silica core
Polymer functionalization
UnaG protein
Bilirubin
Polyguanidine
Magnetic and fluorescent properties

ABSTRACT

The synthesis of multifunctional nano-sized materials is leading to the rapid development of key application, including improved drug delivery, bioimaging and protein separation. In this work, magnetic silica particles modified with novel guanidine containing co-polymers were manufactured via sol-gel method. To evaluate the chemical composition of our prepared samples, FT-IR spectroscopy and thermogravimetry were conducted. Scanning electron microscopy was used in order to investigate the morphology of final products after modification by guanidine containing co-polymers and iron nanoparticles. In addition, the surface of polymer-silica composites was functionalized by the novel bilirubin-inducible fluorescent protein UnaG. In an aqueous bilirubin solution, the silica particles decorated with the polymer-UnaG have showed bright fluorescence. Synthesis and characterization of these hybrid materials allow developing of new multifunctional nano-sized materials, which will be used for detection and separation of bilirubin, a lipophilic heme catabolite that is a clinical diagnostic for liver function.

1. Introduction

It is well known that the surfaces of nano-sized materials have high free energy providing high reactivity. Therefore, the surfaces of nanoparticles will adsorb biomolecules when it comes into

* Corresponding author. Inorganic Chemistry Department, Ivanovo State University of Chemistry and Technology (ISUCT), 7, Sheremetevsky prosp., 153000, Ivanovo, Russian Federation.
E-mail address: a_timin@mail.ru (A.S. Timin).

http://dx.doi.org/10.1016/j.matchemphys.2016.08.048
0254-0584/

contact with biological fluids [1–3]. As a result, the interaction between nanoparticles and biological cells can lead to dysfunction of metabolism of these cells and, therefore, a high toxicity of nanoparticles can damage and destroy the cells. Despite this fact, many types of nanomaterials due to their unique characteristics inherent to the nanoscale can be effectively used for targeting of different proteins and anticancer drugs [4–6]. It makes them relevant for application in nanomedicine as protein/DNA or anticancer drug carriers. Various nanomaterials have been widely investigated for potential application in drug delivery systems. Different metallic nanoclusters based on gold, iron, silver nanodots and its hybrids have found potential application for targeting cancer drugs [7–9]. However, the effect of toxicity of nanoparticles has seriously limited their application in the biological media, for example, in blood plasma. In order to reduce nanoparticles toxicity several methods of surface coating have been suggested.

These methods are based on biomolecular grafting using antibodies, proteins, DNAs that are specially designed for targeting in nanomedicine [10,11]. However, it worth emphasizing that different polymers with biological properties are used for surface modification. A number of polymers have been already synthesized and applied for surface modification of nanoparticles. The most commonly studies include poly (acrylamide) [12], polyethilenglycol [13], polyacrilic acid [14]. The silica nanoparticles have gained much importance for polymer grafting. Due to high chemical and excellent biocompatibility, silica nanoparticles interacting with polymers can form « core-shell » structure which consists of silica core and polymeric shell (Fig. 1a) [15].

Functional groups of polymers provide interactions between surface of polymer coated nanoparticles with proteins, anticancer drugs and biological samples via van der Waals and electrostatic binding [16]. In this field, a new kind of polymers should be examined for developing of new surface properties of polymer coated nanoparticles. Taking into account previously published results, we can consider guanidine containing polymers as one of the most promising candidates for surface modification due to their non-toxicity, biological activity and high binding ability [17,18]. Our recent studies are focused on application of these polymers and its analogues for surface modification of silica nanoparticles. For example, it has been recently demonstrated that polymethacryloyl guanidine hydrochloride (PMCGH) and polyacrylate guanidine (PAG) can be considered for modification of silica nanoparticles with formation of «core-shell » structure and further application of polymer coated silica nanoparticles as drug carriers and hemoadsorbents [19,20]. Herein, we used new type of guanidine containing copolymers: methacrylate guanidine with dialdehyde cellulose (MAG + DAC); diallyl dimethyl ammonium chloride with diallyl guanidine acetate (DDAC + DGA, 75:25) (Fig. 1c, d). Besides, it was reported that guanidine fragment in polymeric chain is more promising than their amine equivalents due to capability of guanidine groups bind stronger with negative molecules compared to amine groups [21].

Today all researchers in the field of nanotechnology concentrate on synthesis of multifunctional nanoparticles with multiple properties, such as fluorescence and magnetics. The potential of fluorescent nanoparticles in biomedical applications is enormous [22,23]. Nanoparticles are effectively rendered fluorescent by immobilizing fluorescent proteins onto their surface [22]. As traditional fluorescent proteins, *Aequorea* GFPs [24] and GFP-like proteins [25] are well-known. However, Miyawaki and his colleagues have achieved the molecular cloning and characterization of a new type of fluorescent protein from the Japanese eel (Fig. 1e). This protein, called UnaG, becomes fluorescent when it forms a special complex with bilirubin (BR). Although being a dicarboxylic acid (Fig. 1b), BR is a water-insoluble molecule; it adopts a "ridge-tile" conformation in solution to make intramolecular hydrogen bonds that prevent the two propionic acid groups from interacting with water. While circulating in human blood plasma, BR is bound to serum albumin [27]. It is transported to the liver, where it is normally conjugated with glucuronic acid to become water-soluble and excreted into bile [20]. BR may be accumulated in blood at high concentrations once patients suffer from a liver disease (hyperbilirubinemia) [21]. Thus, serum levels of BR are a key factor for identification of liver disease. In the past, various biochemical methods based on determination of total bilirubin in blood samples by colour have been used. Usually, it is used UV–Visible spectroscopy for determination of bilirubin concentration. However, all of these methods are not so effective because of the influence of other components in blood (for example, albumins) on UV–Vis spectra of bilirubin absorption. Therefore, to search new effective methods of bilirubin detection is still actual and relevant [28–30]. As it was already mentioned that UnaG protein can show fluorescence when it binds to BR that emphasizes the actual interest of application of UnaG protein for BR due to fluorescent properties of its complex.

In this study, we prepared polymer-coated silicas with γ-Fe_2O_3 nanoparticles and guanidine containing copolymers for further functionalization by Unag protein. This paper points out magnetic properties of prepared samples and fluorescent properties of complex of UnaG-BR on the silica surface.

2. Experimental section

2.1. Chemicals

TEOS ($Si(OC_2H_5)_4$, $M_w = 208.3$ g/mol, 99%) and ammonia solution (30 wt% and 4 wt%) were purchased from commercial chemical company "Ecos-1" (Russian Federation). $FeCl_3$ ($M_w = 162.2$ g/mol, 99%), $FeCl_2$ ($M_w = 126.7$ g/mol, 98%) and BR ($M_w = 584.7$ g/mol) were purchased from Sigma-Aldrich (USA). Bilirubin-bovine serum albumin (BR-Albumin) complex and phosphate buffer (1–1) obtained from "AGAT-MED" (Russian Federation). The guanidine containing polymers: copolymer of methacrylate guanidine and dialdehyde cellulose (MAG + DAC); copolymer of diallyl dimethyl ammonium chloride with diallyl guanidine acetate (DDAC + DGA, 75:25) were provided by the department of macromolecular compounds of the Kabardino-Balkar State University and by the department of Chemistry of polyelectrolytes and biomedical polymers of A.V. Topchiev Institute of Petrochemical Synthesis, Russian Academy of Science. The full description of these guanidine containing copolymers can be found in Refs. [31,32]. Protein samples of apoUnaG were obtained from Brain RIKEN Science institute, Japan. The structure of UnaG and fluorescent properties of UnaG-BR can be found in Ref. [26]. All chemicals were analytical grade and used without further treatment.

2.2. Synthesis of MAG + DAC-SNP-γ-Fe_2O_3 and DDAC + DGA-SNP-γ-Fe_2O_3

The magnetite (γ-Fe_2O_3) was prepared using co-precipitation method with further thermal treatment at 250 °C [33,34]. Briefly, aqueous solution of $FeCl_3$ and $FeCl_2$ was prepared in 2:1 ratio. 203 mg of $FeCl_3$ and 79 mg of $FeCl_2$ were put in 25 mL of aqueous solution. 30% Ammonia solution was added to this solution to make pH = 10. The temperature of solution was increased up to 90 °C. After being rapidly stirred for 4 h the solution became black indicating the formation of Fe_3O_4. The black solution was filtered, washed with water and ethanol several times, and then the black powder was thermally treated at 250 °C for 2 h. During thermal treatment the black powder (Fe_3O_4) was transformed into reddish-brown colored powder (γ-Fe_2O_3). The powder of γ-Fe_2O_3 was further characterized by XRD analysis in order to confirm the formation of gamma phase of Fe_2O_3. The obtained γ-Fe_2O_3 was used in

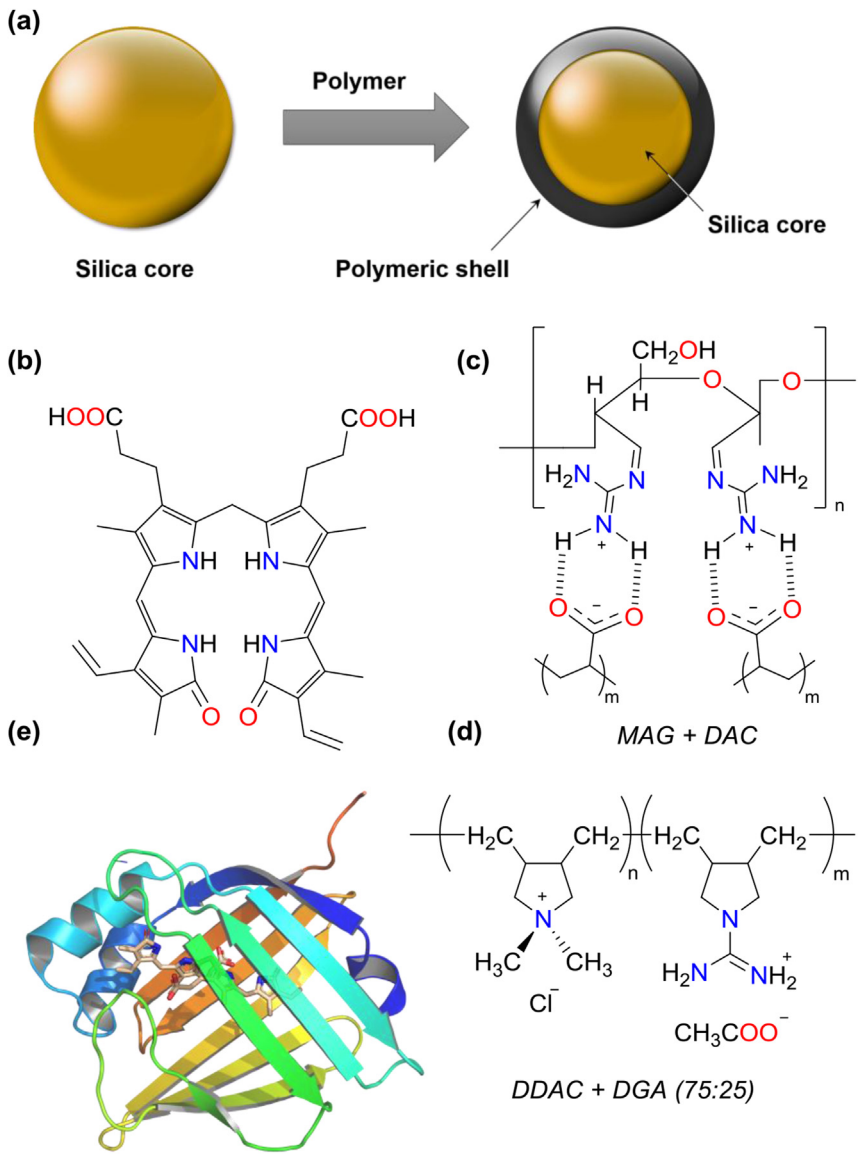

Fig. 1. (a) Schematic illustration of silica core modification by polymer coating; (b) structure of bilirubin IXα; (c) UnaG (wild type, pdb.org No. 4I3B) protein crystal structure; (d) structures of MAG + DAC and (e) DDAC + DGA (75:25).

sol-gel synthesis of silica composite materials. For this reason, 90 mg of γ-Fe_2O_3 was mixed with 4.5 mL of H_2O containing from 0.1 to 0.3 g of polymer in order to form solution A (20 mg/mL of γ-Fe_2O_3 and 22–66.6 mg/mL of guanidine containing co-polymers). After that, the solution A was added to solution B (6 g of TEOS and 1 mL of H_2O) and vigorously stirred until homogeneous mixture was being obtained. Then, the solution was stirred for 6 h. 1.5 μL of aqueous ammonia solution (4 wt %) was added every 30 min as a catalyst. Finally, the obtained product was washed several times and dried under vacuum at 96 °C for 24 h. Thus, the samples with the lowest and highest amount of grafted polymer were prepared, respectively. The same procedure was repeated for non-modified silica (SNP-γ-Fe_2O_3) in the absence of polymers. For polymer coated silica particles we have following abbreviation: MAG + DAC-SNP-γ-Fe_2O_3 and DDAC + DGA-SNP-γ-Fe_2O_3.

2.3. Preparation of UnaG, BR and BR-Albumin solutions

Protein samples of apoUnaG and BR-Albumin complex were dissolved in ultra-pure water. BR solution was prepared by dissolving in 100 μL of NaOH solution, followed by adjusting the pH to 7.4 to obtain the initial concentration 1 mM.

2.4. Functionalization of silica composites by UnaG

The polymer-coated silica composite materials with γ-Fe_2O_3 nanoparticles were further functionalized by UnaG using an adsorption method [33]. It was based on two stages: the deposition of apoUnaG with BR and direct holoUnaG adsorption. In both cases, at first stage a bulk material (25 mg of solid sample) was incubated in a 2 mL solution containing 0.99 μM holoUnaG or apoUnaG.

In case of apoUnag, after vigorous mixing for 5 min and centrifugation (6000 rpm) for 5 min at 4 °C, the precipitate was put into a BR solution (2 mL, c (BR) = 2.16 μM), while supernatant was also mixed with BR. All solid samples with adsorbed UnaG/BR were separated from the solution and prepared for fluorescent microscopy while supernatant was additionally analysed by fluorescence spectroscopy.

In case of holoUnaG, after adsorption procedure and centrifugation for 5 min at 4 °C and 6000 rpm, solid samples with adsorbed holoUnaG were prepared for fluorescent microscopy while supernatant was additionally analysed by fluorescence spectroscopy.

2.5. Characterization

2.5.1. Scanning electron microscopy

The images of uncoated and polymer coated silica particles were obtained using LEO 1550 Scanning Electron Microscope (SEM) which is available in Centre of MicroNano Technology (CMi) of Ecole Polytechnique Fédérale de Lausanne (EPFL). Before examining, all samples were mixed with ethanol to prepare suspension. The drop of the suspension was adhesive onto copper surface and dried. SEM imaging was performed under a working distance between 3 and 4 mm with acceleration voltages of 3–5 kV. The chamber vacuum was 10^{-7} mbar. We used SE2 signal (topography visualization) for SEM imaging.

2.5.2. Fourier transform infrared (FT-IR) spectroscopy

FT-IR spectra of the samples were recorded on a Nicolet TM 4700 FTIR spectrometer ("Nicolet", USA) using KBr technique.

2.5.3. X-ray diffraction (XRD) analysis

XRD patterns were recorded under a Bruker X-ray diffractometer D8 Advance using Cu-K_α radiation over the range $10^\circ \leq 2\theta \leq 70^\circ$.

2.5.4. Thermal gravimetric (TG) analysis

TG analysis was used to determine the content of grated polymer into silica core and conducted via STA 449 F3 Jupiter (Netzsch, Germany) in argon atmosphere from room temperature up to 900 °C with a ramp rate of 10 °C/min. An alumina crucible with a cover was used during thermal analysis.

The amount of grafted co-polymers has been calculated using following equation:

$$\text{Grafting yield}(\text{GY, }\%) = \frac{W_1 - W_0}{W_0} \times 100$$

where W_1 and W_0 represent the weight loss of initial and grafted substrate, respectively.

2.5.5. Fluorescence spectroscopy

Fluorescence spectra were obtained on the fluorescence spectrometer Cary-Agilent Eclipse. The detection rate of spectra was 1200 nm/min at 600 V (detector voltage). The width of the excitation and emission slits was 5 nm in all cases. All experiments were carried out at 298 ± 1 K in a thermostatic cell equipped with a Peltier heat-transfer module. The investigations were carried out in quartz cuvettes with light-absorbing layer thickness of 1 cm. All experiments were performed in phosphate buffer at pH 7.4. Excitation wavelength was 498 nm.

2.5.6. Fluorescence microscopy

Images were obtained using Live Imaging System based on Olympus IX81 fluorescent microscope (magnification ×20/0.5) equipped with a GFP (FITC/Cy2-494/518) filter set and a motorized stage. Samples were placed between hydrophobic glass plates. DuPont™ Elvanol® (polyvinyl alcohol) was used as adhesive to avoid bubbles formation.

2.5.7. Vibrating-sample magnetometer

A vibrating-sample magnetometer (VSM) (EG & G Princeton Applied Research vibrating sample magnetometer, model 155) was used at 300 K to measure the magnetic moment.

3. Results and discussion

3.1. Preparation of MAG + DAC-SNP-γ-Fe_2O_3 and DDAC + DGA-SNP-γ-Fe_2O_3

The γ-Fe_2O_3 nanoparticles were prepared using well-known co-precipitation method [33,34]. After that, the reddish-brown coloured solution of γ-Fe_2O_3 nanoparticles with concentration of 20 mg/mL was added slowly to sol-gel solution containing TEOS and guanidine co-polymers. The obtained mixture was stirred until silica particles were formed. Then, we have characterized the obtained silica composites having low and high amount of guanidine containing co-polymers.

First of all, TG analysis was performed in order to evaluate the grafting amount of guanidine containing co-polymers (Supporting information, Fig. 1S). According to the obtained TGA curves, it was determined that the maximum grafting yield for MAG + DAC-SNP-γ-Fe_2O_3 and DDAC + DGA-SNP-γ-Fe_2O_3 does not exceed 29.72–30.79%. Herein, we focus on investigation of samples with maximum grafting content of co-polymers because the immobilization of biocompatible polymers such as guanidine containing co-polymers can protect against toxic effect of nanoparticles [1–3]. Therefore, the samples with maximum content of guanidine containing co-polymers were further studied.

Powder X-ray diffraction (XRD) patterns were analysed for γ-Fe_2O_3 nanoparticles and silica composite materials (Supporting information, 2S). The silica composite materials (MAG + DAC-SNP-γ-Fe_2O_3 and DDAC + DGA-SNP-γ-Fe_2O_3) show a broad diffraction peak at 22.5 °C corresponding to the amorphous silica (JCPDS: 29–0085) and several diffraction peaks which are assigned to γ-Fe_2O_3 (maghemite, JCPDS: 39–1346). FT-IR spectroscopy was conducted to determine the presence of functional groups of grafted polymers after sol-gel modification. FT-IR spectra of pure guanidine containing copolymers (MAG + DAC, DDAC + DGA) are presented in Supporting information, Fig. 3S. According to FT-IR spectra of prepared silica composite materials: SNP-γ-Fe_2O_3, MAG + DAC-SNP-γ-Fe_2O_3 and DDAC + DGA-SNP-γ-Fe_2O_3 (Fig. 2) several peaks can be observed which correspond to the chemical bonds of silica and guanidine containing co-polymers. A broad band in the range 3600–3300 cm^{-1} can be assigned to the O–H stretching bands of hydrogen-bonded water molecules and SiO–H stretching vibrations [35]. The corresponding Si–OH bending mode is found around 950 cm^{-1}. The "bulk" vibrational modes corresponding to SiO_4 groups are observed at 1087–1095 cm^{-1} and 800 cm^{-1} (antisymmetric and symmetric Si–O–Si vibrations, respectively), with the bending vibrations near to 460 cm^{-1} [36]. It is clearly seen that after sol-gel modification the FT-IR spectra polymer coated silicas have shown new frequencies corresponding to the functional groups in guanidine containing copolymers. In case of DDAC + DGA-SNP-γ-Fe_2O_3 the band around 1649 cm^{-1} can be assigned to the combination of N=C, NH_2 and H–O vibrations. The intensive peak at 1561 cm^{-1} corresponds to the CH_3COO^- vibrations in DDAC + DGA. The bands between 3000 and 2800 cm^{-1} correspond to intensive asymmetric and symmetric C–H stretching vibrations of methylene and methane groups in DDAC + DGA. As for MAG + DAC-SNP-γ-Fe_2O_3 it can be observed two most intensive peaks at 1538 and 1662 cm^{-1} respectively. The first one can be assigned to C=O groups in MAG + DAC and second one is associated with N–H vibrations. Perceptible differences were observed in 1500–1350 cm^{-1} region which is responsible for carboxylic and amine bonds in guanidine containing copolymers. FT-IR spectra also give us the information about the presence of γ-Fe_2O_3 in our samples. From the spectra, it can be seen that two broad peaks at

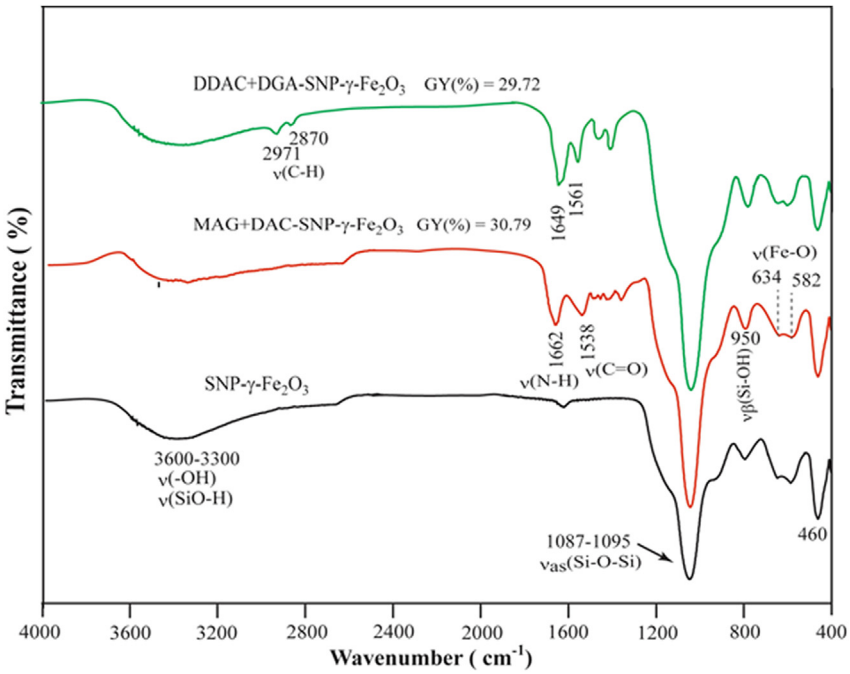

Fig. 2. FT-IR spectra of uncoated and polymer coated silica particles.

555 and 463 cm^{-1} were identified. These peaks correspond to Fe–O stretching and bending vibration mode of γ-Fe_2O_3 [37]. Thus, FT-IR spectroscopy has also shown the presence of guanidine containing copolymers and γ-Fe_2O_3 in our samples after sol-gel synthesis and consequently confirms silica modification by these chemical components.

The SEM analysis was used in order to reveal any morphological changes after sol-gel modification. The results of SEM analysis are presented in Fig. 3. It is clearly seen that non-modified silica had non-uniform spherical shape. The particles with mean diameter of 200 nm as well as the particles with mean diameter of 350–410 nm can be detected. As it was reported previously [38], the morphology, shape and size of particles depend on sol-gel conditions: pH value, reaction time, temperature, concentrations of initials reagents and addition of surfactants. Considering obtained results, the sol-gel synthesis of non-modified silica allows to prepare non-uniform silica particles with wide size distribution. The SEM image of γ-Fe_2O_3 nanoparticles was shown in Fig. 3b for the comparison. The average size of γ-Fe_2O_3 is around 18–21 nm. As it can be seen from Fig. 3 (c, d), MAG + DAC-SNP-γ-Fe_2O_3 and DDAC + DGA-SNP-γ-Fe_2O_3 have slightly distorted spherical shape with multiple white spots (γ-Fe_2O_3) around silica particles. Moreover, the particle size of MAG + DAC-SNP-γ-Fe_2O_3 (~120–175 nm) and DDAC + DGA-SNP-γ-Fe_2O_3 (~140–210 nm) is lower in comparison with non-modified silica. Such changes in morphology of polymer-silica composites confirm successful sol-gel modification. Also the nanosized characteristics are so critical when these materials are further considered for biological application.

Magnetic properties of γ-Fe_2O_3 and polymer-silica composites were studied. The magnetic hysteresis curves were recorded at 300 K (room temperature) (Fig. 4)a. According to Fig. 4a, the saturation magnetization of γ-Fe_2O_3 is 51.3 emu/g. The magnetic intensity of DDAC + GA-SNP-γ-Fe_2O_3 (21.5 emu/g) and MAG + DAC-SNP-γ-Fe_2O_3 (29.1 emu/g) are lower than γ-Fe_2O_3 due to the presence of non-magnetic components (silica and guanidine containing co-polymers) [38]. Nevertheless, polymer-silica composites exhibit supermagnetic state at room temperature which is desirable for many practical applications. Moreover, MAG + DAC-SNP-γ-Fe_2O_3 dispersed in water solutions can be separated from water by suing a typical hand-held magnet (Fig. 4b, Supporting information, Video 1). Also it should be noted that interactions of γ-Fe_2O_3 with surface of polymer-silica composites are strong enough in order to perform a motion of polymer-silica composites under the influence of magnetic field.

Supplementary video related to this article can be found at http://dx.doi.org/10.1016/j.matchemphys.2016.08.048.

3.2. Fluorescent properties of magneto-polymer coated silicas after functionalization by UnaG-BR complex

In the previous study by Kumagai et al. [26], DMSO was used to prepare a stock solution of BR, which is water-insoluble. After dilution with phosphate buffer (pH 7.4), BR solutions were mixed with apoUnaG to construct holoUnaG. Then, DMSO and free BR were removed by gel-filtration. In this study, by contrast, we employed a simplified procedure for holoUnaG preparation that used no DMSO.

We performed the titration of BR solution by adding experimentally-determined concentrations of apoUnaG to study fluorescent properties of the holo UnaG in aqueous solution (pH 7.4). Immediately after the addition, we observed a substantial increase in fluorescence, whose spectra were identical to those previously presented in Ref. [26] (Fig. 5a). The fluorescence value did not change after 2 weeks at 4 °C, which confirmed the high stability of holoUnaG complex.

Then, we have studied the influence of the carrier protein albumin on binding ability between apoUnaG and BR. It can be observed the similar increase in fluorescent spectra in the presence of BSA (Fig. 5c). However, it is required less concentration of apoUnaG (in 6 times lower) to reach the same fluorescence value compared to free BR. This fact might be associated with higher solubility of BR in the presence of albumin due to the formation of BR-Albumin complex. The K_d constant values for BR-apoUnaG (98 pM) are lower than in case of BR-albumin (18 μM [39]). As a result, the BR-UnaG complex is much more stable than BR-bovine serum albumin. These results indicated that such small concentrations

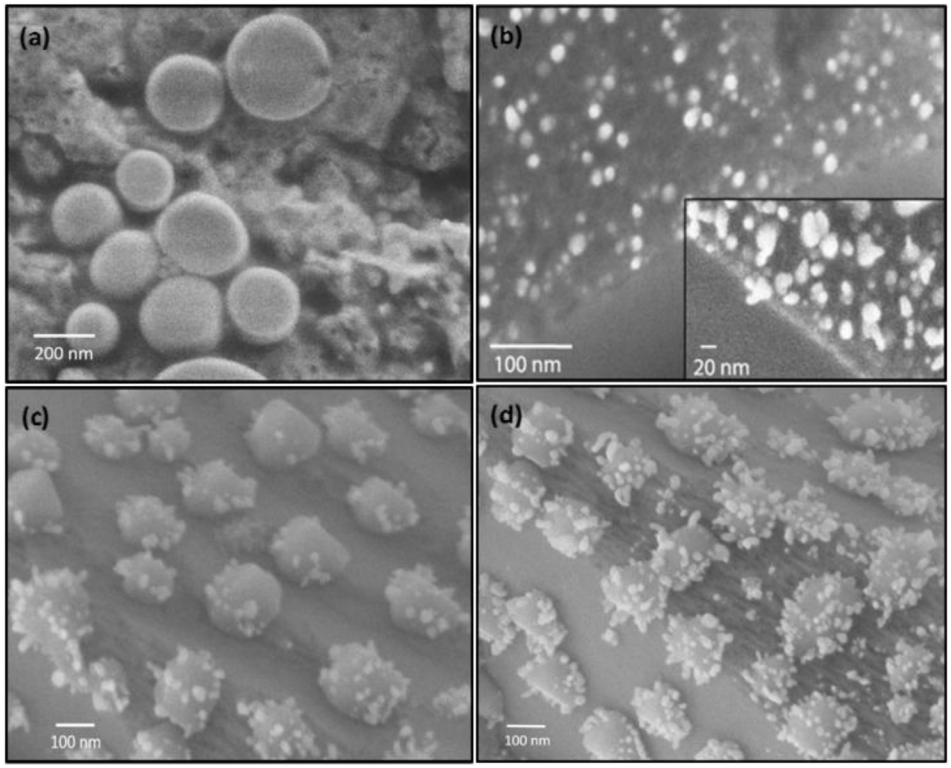

Fig. 3. SEM image of (a) non-modified silica, (b) γ-Fe_2O_3 nanoparticles, (c) DDAC + DGA-SNP-γ-Fe_2O_3 and (d) MAG + DAC-SNP-γ-Fe_2O_3 respectively.

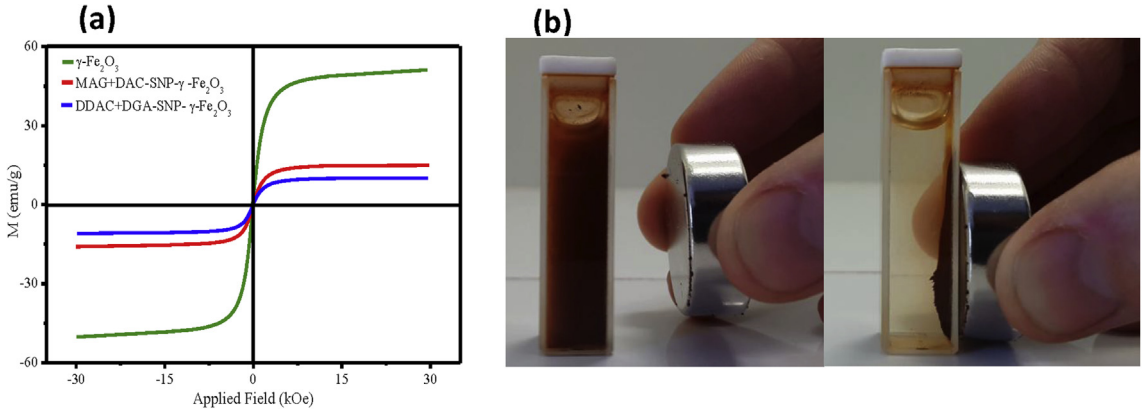

Fig. 4. (a) Hysteresis curves of γ-Fe_2O_3 (green line), MAG + DAC-SNP-γ-Fe_2O_3 (red line) and DDAC + GA-SNP-γ-Fe_2O_3 (blue line) at 300 K; (b) MAG + DAC-SNP-γ-Fe_2O_3 composite dispersed water solution and magnetic separation. (For interpretation of the references to colour in this figure legend, the reader is referred to the web version of this article.)

(micro- and nanomolar) of apoUnaG are enough for BR detection in aqueous solution using fluorescent spectroscopy.

The next stage was to the fluorescence of polymer coated samples after holoUnag functionalization. For this reason we performed adsorption technique. It is clearly seen that after even 10 min of adsorption, the fluorescence intensity of holoUnaG in solution was decreased by 2 times (Fig. 5d).

According to images of fluorescent microscope (Fig. 5e), non-modified silica particles did not show fluorescence. However, at the same time after functionalization of holoUnag polymer coated silica particles we can observe green fluorescence of polymeric shell due to the protein-BR adsorbed onto the surface. We suppose that the binding of the protein occurs via electrostatic forces. The fluorescence intensity of MAG + DAC-SNP-γ-Fe_2O_3 is slightly higher in comparison with DDAC + GA-SNP-γ-Fe_2O_3. To sum up, we can conclude that holoUnaG with BR does not unfold and becomes stable even after adsorption forming fluorescent complex with BR molecules. Here we have shown the potential application of UnaG for bilirubin detection in aqueous solution in the presence of albumin and on the surface of polymer coated particles. These results can be interesting for development of new methods of bilirubin detection and further removal from blood plasma using functional modified silica nanoparticles.

4. Conclusions

The magneto-polymer coated silica particles have been synthesized via sol-gel method. The incorporation of γ-Fe_2O_3

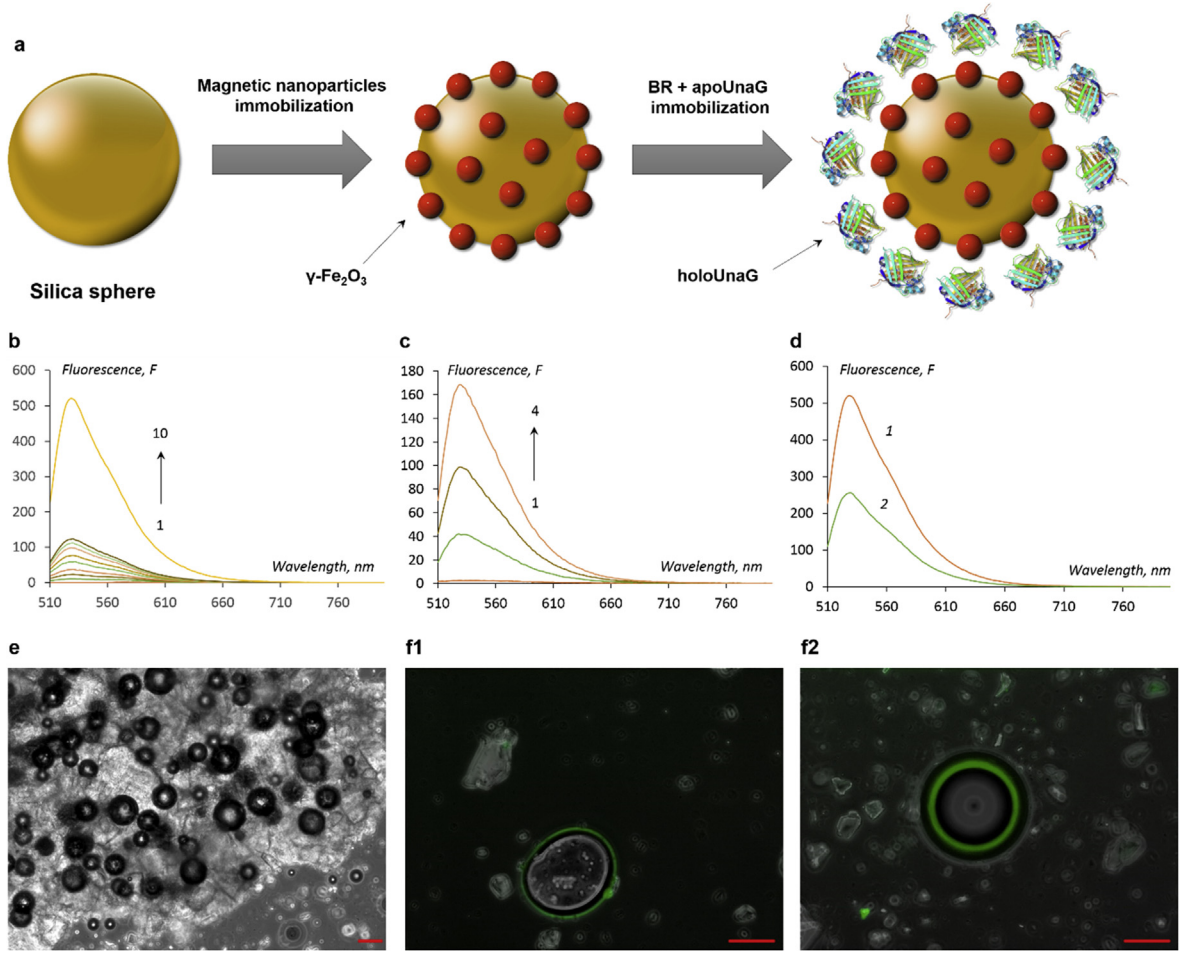

Fig. 5. (a) Scheme of preparation of fluoromagnetic UnaG-BR (holoUnaG)-containing silica particles (b) The increase in fluorescence after titration of BR ($c_0 = 1$ μM, 1) with apoUnaG (c, μM:1–0, 2–0.27, 3–0.55, 4–0.82, 5–1.09, 6–1.36, 7–1.63, 8–1.90, 9–2.16, 10 – through 5 days). (c) The increase in fluorescence after titration of BR-Albumin complex ($c_0 = 1$ μM, 1) by UnaG (c, μM:1–0, 2–0.27, 3–0.55, 4–0.82). (d) The fluorescence difference amongst the sample before (1) and after (2) adsorption of holoUnaG on magneto-polymer coater silica particles. (e) Fluorescent microscopy images of sample without UnaG (SNP-γ-Fe_2O_3) (non-fluorescent) and with holoUnag – DDAC + GA-SNP-γ-Fe_2O_3 (f1) and MAG + DAC-SNP-γ-Fe_2O_3 (f2) (green fluorescence). (For interpretation of the references to colour in this figure legend, the reader is referred to the web version of this article.)

nanoparticles allowed to provide magnetic properties of our samples and, therefore, separation of particles by the influence of magnetic field. Despite the fact that the silica was chosen as a core for polymer coating, we should emphasize that other available matrixes based on titania, carbon, graphene oxide can be easily used for surface functionalization with guanidine polymers. Therefore, we expect that such guanidine containing polymers could be further considered in wide range of affinity systems. A new type of magnetic polymer coated nanoparticles containing unique ligand-switching protein UnaG were also obtained. Established that bilirubin-contained holoUnaG protein being adsorbed on magnetic silica particles keeps their high intrinsic fluorescence. Such composite may be applied for bilirubin detection and removal using magnetic field.

Acknowledgements

This work was partially supported by Russian Foundation for Basic Research grants No. mol_a 16-33-00966 (2016–2017), 15-43-03214 r_center_a (2015–2016), 15-33-20002 mol_a_ved (2015–2016) and 15-33-50321 mol_nr (2015–2016).

We also thank Dr. Aleksandra Radenovic (Laboratory of Nanoscale Biology, EPFL, Lausanne, Switzerland) and Centre Interdisciplinaire de Microscopie Electronique (CIME) at EPFL for access to electron microscope (SEM); Dr. Tomer Zidki and Dr. Hana Okhrimenko (Ariel University Center of Samaria, Biological Chemistry Department, Ariel, Israel) for providing us the fluorescent microscope.

Appendix A. Supplementary data

Supplementary data related to this article can be found at http://dx.doi.org/10.1016/j.matchemphys.2016.08.048.

References

[1] T. Cedervall, I. Lynch, S. Lindman, T. Berggård, E. Thulin, H. Nilsson, K.A. Dawson, S. Linse, Understanding the nanoparticle–protein corona using methods to quantify exchange rates and affinities of proteins for nanoparticles, Proc. Natl. Acad. Sci. U. S. A. 104 (2007) 2050–2055.
[2] A. Nel, L. Mädler, D. Velegol, T. Xia, E.M.V. Hoek, P. Somasundaran, F. Klaessig, V. Castranova, M. Thompson, Understanding biophysicochemical interactions at the nano–bio interface, Nat. Mater 8 (2009) 543–557.
[3] I. Lynch, K.A. Dawson, Protein–nanoparticle interactions, Nano Today 3 (2008) 40–47.
[4] Y. Piao, A. Burns, J. Kim, U. Wiesner, T. Hyeon, Designed fabrication of silica-based nanostructured particle systems for nanomedicine application, Adv. Funct. Mater 18 (2008) 3745–3758.
[5] E. Busseron, Y. Ruff, E. Moulin, N. Giuseppone, Supramolecular self-assemblies as functional nanomaterials, Nanoscale 5 (2013) 7098–7140, http://dx.doi.org/10.1039/c3nr02176a.

[6] K. Rudzka, J.L. Viota, J.A. Munoz-Gamez, A. Carazo, A. Ruiz-Extremera, A.V. Delgado, Nanoengineering of doxorubicin delivery systems with functionalized maghemite nanoparticles, Colloids Surf. B Biointerfaces 111 (2013) 88–96.
[7] W. Qi, M. Shen, T. Zhao, Y. Xu, J. Lin, Y. Duan, H. Gu, Low toxicity and long circulation time of polyampholyte-coated magnetic nanoparticles for blood pool contrast agents, Sci. Rep. 5 (2015) 7774, http://dx.doi.org/10.1038/srep07774.
[8] Y.H. Jang, Y.J. Jang, S.T. Kochuveedu, M. Byun, Z. Lin, D.H. Kim, Plasmonic dye-sensitized solar cells incorporated with $AuTiO_2$ nanostructes with tailored configurations, Nanoscale 6 (2014) 1823, http://dx.doi.org/10.1039/C3NR05012B.
[9] A. Baeza, E. Guisasola, E. Ruiz-Hernández, M. Vallet-Regí, Magnetically triggered multidrug release by hybrid mesoporous silica nanoparticles, Chem. Mater 24 (2012) 517–524.
[10] M. Ferrari, Cancer nanotechnology: opportunities and challenges, Nat. Rev. Cancer 5 (2005) 161–171.
[11] M.T. Stephan, J.J. Moon, S.H. Um, A. Bershteyn, D.J. Irvine, Therapeutic cell engineering with surface-conjugated synthetic nanoparticles, Nat. Med. 16 (2010) 1035–1041.
[12] S. Baljit, G.S. Chauhan, S. Kumar, N. Chauhan, Synthesis, characterization and swelling responses of pH sensitive psyllium and polyacrylamide based hydrogels for the use in drug delivery, Carbohydr. Polym. 67 (2007) 190–200.
[13] K. Knop, R. Hoogenboom, D. Fischer, U.S. Schubert, Poly(ethylene glycol) in drug delivery: pros and cons as well as potential alternatives, Angew. Chem. Int. Ed. 49 (2010) 6288–6308.
[14] C. Müller, K. Leithner, S. Hauptstein, F. Hintzen, W. Salvenmoser, A. Bernkop-Schnürch, Preparation and characterization of mucus-penetrating papain/poly(acrylic acid) nanoparticles for oral drug delivery applications, J. Nanoparticle Res. 15 (2013) 1353.
[15] H. Zou, W. Sh, J. Shen, Polymer/silica nanocomposites: preparation, characterization, properties, and applications, Chem. Rev. 108 (2008) 3893–3957.
[16] S. Dufort, L. Sancey, J.L. Coll, Physico-chemical parameters that govern nanoparticles fate also dictate rules for their molecular evolution, Adv. Drug Deliv. Rev. 64 (2012) 179–189.
[17] K.E. Locock, T.D. Michl, J.D. Valentin, K. Vasilev, J.D. Hayball, Y. Qu, A. Traven, H.J. Griesser, Guanylated polymethacrylates: a class of potent antimicrobial polymerswith low hemolytic activity, Biomacromolecules 14 (2013) 4021–4031.
[18] A.S. Timin, A.V. Solomonov, E.V. Rumyantsev, Polyacrylate guanidine and polymethacrylate guanidine as novel cationic polymers for effective bilirubin binding, J. Polym. Res. 21 (2014) 400–409.
[19] A.S. Timin, S.Yu Khashirova, A. Zhansitov, E.V. Rumyantsev, Synthesis and application of silica hybrids grafted with new guanidine-containing polymers as highly effective adsorbents for bilirubin removal, Colloid Polym. Sci. 293 (2015) 1667–1674.
[20] A.S. Timin, E.V. Balantseva, A. Zhansitov, E.V. Rumyantsev, T.Yu Osadchaya, Application of guanidine-containing polymers for preparation of pH responsive silica-based particles for drug delivery systems, Colloids Surfaces A Physicochem. Eng. Aspects 477 (2015) 26–34.
[21] A.M. Carmona-Ribeiro, L.D. Melo Carrasco, Cationic antimicrobial polymers and their assemblies, Int. J. Mol. Sci. 14 (2013) 9906–9946, http://dx.doi.org/10.3390/ijms14059906.
[22] M.J. Ruedas-Rama, J.D. Walters, A. Orte, E.A.H. Hall, Fluorescent nanoparticles for intracellular sensing: a review, Anal. Chim. Acta 751 (2012) 1–23.
[23] M.A. Rizzo, M.W. Davidson, W. David Piston, Fluorescent protein tracking and detection: applications using fluorescent proteins in living cells, Cold Spring HarbProtoc (2009), http://dx.doi.org/10.1101/pdb.top64.
[24] R.Y. Tsien, The green fluorescent protein, Annu. Rev. Biochem. 67 (1998) 509–544.
[25] D.M. Chudakov, M.V. Matz, S. Lukyanov, K.A. Lukyano, Fluorescent proteins and their applications in imaging living cells and tissues, Physiol. Rev. 90 (2010) 1103–1163.
[26] A. Kumagai, R. Ando, H. Miyatake, P. Greimel, T. Kobayashi, Y. Hirabayashi, T. Shimogori, A. Miyawaki, A bilirubin-inducible fluorescent protein from eel muscle, Cell 153 (2013) 1602–1611.
[27] G. Baydemir, M. Andac, N. Bereli, Selective removal of bilirubin from human plasma with bilirubin imprinted particles, Ind. Eng. Chem. 46 (2007) 2843–2852.
[28] A. Burns, H. Ow, U. Wiesner, Fluorescent core–shell silica nanoparticles: towards "Lab on a Particle" architectures for nanobiotechnology, Chem. Soc. Rev. 35 (2006) 1028–1042.
[29] L. Zhou, J. Yuan, Y. Wei, Core–shell structural iron oxide hybrid nanoparticles: from controlled synthesis to biomedical applications, J. Mater. Chem. 21 (2011) 2823–2840.
[30] M. De, S. Rana, H. Akpinar, O.R. Miranda, R.R. Arvizo, U.H.F. Bunz, V.M. Rotello, Sensing of proteins in human serum using conjugates of nanoparticles and green fluorescent protein, Nat. Chem. 1 (2009) 461–465.
[31] Applied methodologies in polymer research and technology, in: Abbas Hamrang, Devrim Balkose (Eds.), New Biologically Active Composite Materials on the Basis of Dialdehyde Cellulose 5, 2014.
[32] N.A. Sivov, et al., Biocide and toxicological properties of synthesized guanidine containing polymers and their structure, Mod. tendencies Org. Bioorg. Chem. 27 (2008) today and tomorrow.
[33] M. Aliahmad, N.N. Moghaddam, Synthesis of maghemite (γ-Fe_2O_3) nanoparticles by thermal-decomposition of magnetite (Fe_3O_4) nanoparticles, Mater. Sci. 31 (2013) 264–268.
[34] M. Hua, L. Jian, et al., Characterization of γ-Fe_2O_3 nanoparticles prepared by transformation of a-FeOOH, Chin. Sci. Bull. 56 (2011) 2383–2388.
[35] S.R. Saptarshi, A. Duschl, A.L. Lopata, Interaction of nanoparticles with proteins: relation to bio-reactivity of the nanoparticle, J. Nanobiotechnology 11 (2013) 26, http://dx.doi.org/10.1186/1477-3155-11-26.
[36] L.T. Zhuravlev, The surface chemistry of amorphous silica, Colloids Surf. A 173 (2000) 1–38.
[37] R. Mellaerts, J.A.G. Jammaer, M.V. Speybroeck, H. Chen, J.V. Humbeeck, P. Augustijins, G.V. Mooter, J.A. Martens, Langmuir 24 (2008) 8651–8659.
[38] H. Gao, et al., Composite silica nanoparticle/polyelectrolyte microcapsules with reduced permeability and enhanced ultrasound sensitivity, J. Mater. Chem. B 3 (2015) 1888–1897.
[39] J. Zhou, L. Zhou, C. Dong, Y. Fend, S. Wei, J. Shen, X. Wang, Preparation and photodynamic properties of water-soluble hypocrellin A-silica nanospheres, Mater. Lett. 62 (2008) 2910–2913.